

Motion Artifact Resilient SCG-based Biometric Authentication Using Machine Learning

Po-Ya Hsu,¹ Po-Han Hsu,¹ Tsung-Han Lee¹ & Hsin-Li Liu^{2*}

Abstract—On account of privacy preserving issue and health-care monitoring, physiological signal biometric authentication system has gained popularity in recent years. Seismocardiogram (SCG) is now easily accessible owing to the advance of wearable sensor technology. However, SCG biometric has not been widely explored due to the challenging motion artifact removal. In this paper, we design placing the sensors at different body parts under different activities to determine the best sensor location. In addition, we develop SCG noise removal algorithm and utilize machine learning approach to perform biometric authentication tasks. We validate the proposed methods on 20 healthy young adults. The dataset contains acceleration data of sitting, standing, walking, and sitting post-exercise activities with the sensor placed at the wrists, neck, heart and sternum. We demonstrate that vertical and dorsal-ventral SCG near the heart and the sternum produce reliable SCG biometric evidenced by achieving the state-of-the-art performance. Moreover, we present the efficacy of the devised noise removal procedure in the authentication during walking motion.

Clinical relevance— A seismocardiography-based biometric authentication system can help serve privacy preserving and reveal cardiovascular functioning information in clinics.

I. INTRODUCTION

Today, biometric authentication systems have been widely applied to human identity verification to perform high level security. We illustrate a standard structure in Fig. 1. Typical biometric authentication systems consist of three functional blocks: data cleaning, features processing, and matching evaluation. The matching score will then be utilized to identify the subject's identity. In modern society, face and fingerprint are commonly used biometrics [1]. However, such external biometrics are susceptible to spoofing attacks [2]. For instance, fingerprints are easily left on an object and recreated with latex; facial recognition can be hacked by high-resolution modified photos.

To circumvent the issues in external biometrics, physiological signals such as electrocardiograms (ECG) or seismocardiograms (SCG) has attracted attention as a biometric recently. Both ECG and SCG are continuous measures and reveal quasi-periodic cardiac morphology. ECG measures electrical depolarization and repolarization throughout cardiac activities; SCG captures the chest's surface motion caused by the contraction of the heart [3]. Physiological signals are able to reflect the functioning of an individual's

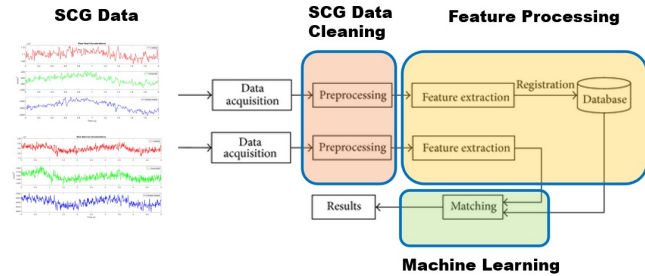


Fig. 1. Schematics of the standard biometric authentication system.

cardiovascular system; furthermore, they show several advantages as a biometric [4]: (1) indicate liveness; (2) difficult to be stolen; (3) easy to acquire with wearable sensors.

ECG has been reported as a promising biometric in several studies [5], [6], yet to the best of our knowledge, the uniqueness of SCG [7] has only been reported in two studies: one is conducted by Bui *et al.* [7], and the other is by Hsu *et al.* [8]. In Bui *et al.*'s work, a 98.89% recognition rate has been reported by manipulating SCG data, but the authentication issue is untouched. In Hsu *et al.*'s study, state-of-the-art SCG biometric performance has been presented, however, it is only adaptable for SCG measured at supine positions.

In this paper, we propose different SCG biometric authentication models adjustable to a person's posture, and we make contributions as follows:

- generate robust SCG biometrics with the devised signal processing procedure
- present state-of-the-art performance motion artifact resilient SCG biometric models

The rest of the paper is organized as follows. We describe the experimental design and SCG model construction in Section II. Subsequently, we present the performance of each proposed SCG biometric authentication model and discuss our experimental results in Section III. Finally, we make conclusions of this work in Section IV.

II. METHODS

We first introduce our experiment design. Following that, we describe the signal processing strategy of the sensor data. Next, we propose our SCG-based biometric models. Last,

This work was not supported by any organization.

¹Po-Ya Hsu, Po-Han Hsu and Tsung-Han Lee are with the Department of Computer Science & Engineering, University of California, San Diego, The USA

²Hsin-Li Liu is with the Department of Nursing, Central Taiwan University of Science and Technology, Taiwan

*Hsin-Li Liu is the corresponding author hlliu@ctust.edu.tw

we specify the performance quantification of the proposed biometric authentication model.

A. Experiment Design

This study was approved by the Jen-Ai Hospital-Joint Institutional Review Board. We recruited 20 young healthy volunteer to undergo the data acquisition process. All 20 subjects voluntarily provided the written informed consent to participate in the study. The age of the participants are 25 – 32 years, and the gender distribution is 6 females and 14 males.

TABLE I
DESIGN OF EXPERIMENTS

Activities	sitting, standing, walking, sitting after walking
Duration	each activity lasts for 3 minutes
Sensor Placements	left/right wrists, heart, sternum, neck near left carotid artery
Description	participants wear the sensors throughout the whole experiment
Sensor	three-axis accelerometers
Measurements	accelerations

We summarize the experimental design in Table I. All the participants went through the four activities: sitting still, standing still, walking at normal pace, and sitting right after walking. For each activity, the participant performs either the same posture or consistent motion (walking) for three minutes with the wearable sensors placed on the body.

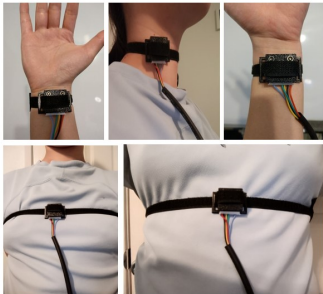


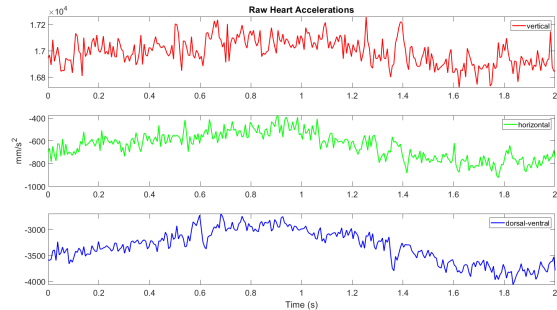
Fig. 2. Demonstration of the sensor placements.

The collected data are body acceleration measured by the wearable sensors. Throughout the whole experiment, the acceleration data are measured with the sensors placed on the participant’s heart, sternum, left carotid, and bilateral wrists (as shown in Fig. 2). These body parts are chosen since it is very likely to measure the heart-induced signals at these locations [9]. The acceleration sensors are MPU-6050, and the data sampling rate is set to 150Hz in our experiment. All the data acquisition was completed by the same person; moreover, before the start of each activity, the person inspected all the sensors to be well-functioning and properly leveled.

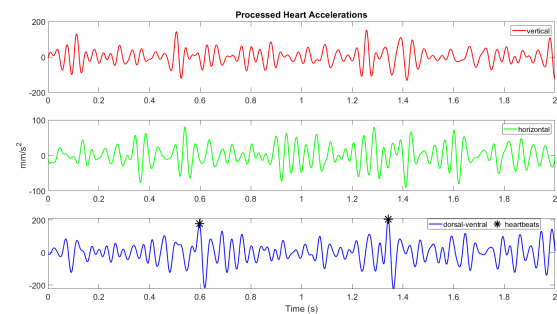
B. Data Processing

We transform the raw acceleration signals into data samples for biometric model construction in five steps: 1) data

normalization, 2) low-frequency noise removal, 3) high-frequency noise removal, 4) data smoothing, and 5) heartbeat peak detection. To be more specific, the whole signal processing procedure is applied to each dimensional acceleration independently. In the first step, we compute the average of each dimensional acceleration and subtract the raw signal by this average so as to remove the gravity effect and other constant acceleration factor, which is known as common average referencing (CAR) and was adopted in [10]. In the second step, we make use of the third order Savitzky-Golay filter to clean the unwanted low-frequency signal. Such approach has been shown effective in removing motion artifact in [11]. In the third step, we remove the high-frequency noise with a sixth-order Butterworth lowpass filter. In the fourth step, we smooth the data through interpolating the processed signal with spline cubic curves at 750Hz. We portrait the raw and processed acceleration signals of the sensor located on top of the heart in Fig. 3. In the final step, we borrow the heartbeat detection technique used in [10] to label the heart pumping peaks in SCG. Herein, the SCGs measured on the heart are employed. Moreover, we chunk the acceleration data into 1-second long SCG centered at the labeled heartbeat peak to standardize the data samples.



(a) Raw SCG



(b) Processed SCG

Fig. 3. Demonstration of the two-second raw and processed SCG data. Red: Vertical; Green: Horizontal; Blue: Dorsal-ventral.

C. Biometric Authentication Model

We devise the SCG-based biometric authentication models considering the following four factors: (1) orientation of the acceleration, (2) locations of the sensor, (3) posture of the human subject, and (4) resilience against motion artifact. For (1), we have 3-axis accelerations for each sensor. Regarding

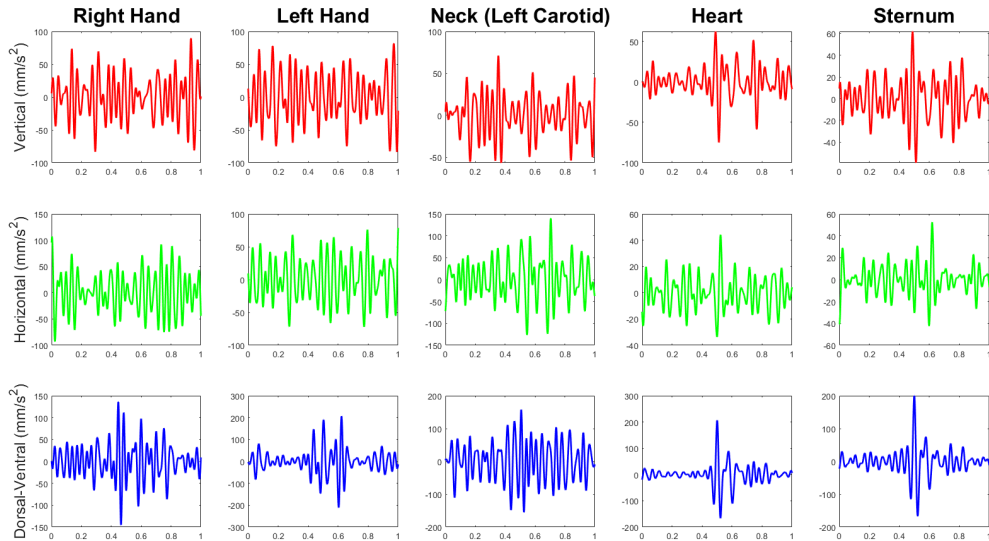


Fig. 4. Demonstration of the 1-second ensemble average SCG waveforms.

(2), we place 5 sensors on different body parts. As for (3), the participants perform 4 different activities, ranging from small movement to large motion. Concerning (4), we leverage the ensemble average trick applied in other SCG studies [12], [3]. To be more specific, instead of using the data sample directly, we remove the motion artifact through averaging five consecutive data samples and build the biometric models using the averaged data. We display the averaged acceleration for building the biometric authentication models in Fig. 4. Consequently, we build a total of 120 models, in which $120 = 3 \times 5 \times 4 \times 2$.

For each model, we adopt support vector machine, a well-known machine learning approach, to learn classifying the twenty subjects' identity based on their processed acceleration data. In our training-testing data segregation, we randomly shuffle the samples and then assign the first 70% as the training dataset with the rest 30% as the testing dataset.

D. Performance Evaluation

For authentication, we assess the performance of the model with the equal error rate (EER), which is the threshold value of false acceptance rate and false rejection rate. EER has been widely known as a standard for the authentication issue.

III. RESULTS & DISCUSSION

We exhibit the EER of each experiment in Table II, and we showcase the competitiveness of the proposed SCG biometric authentication systems in Table III. Our best SCG biometric model is the robust standing heart dorsal-ventral acceleration, which has an EER less than 0.1%. We also plot the training and testing SCG of two subjects in Fig. 5. From the plot, we can clearly perceive the high SCG consistency of the same human participant and dissimilarity of SCG between different people.

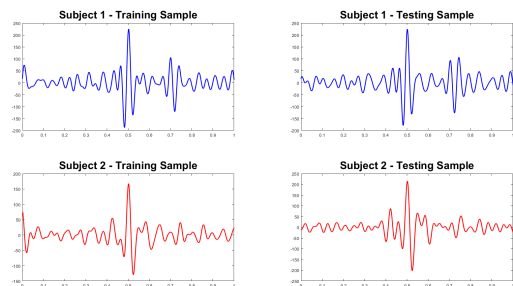


Fig. 5. Demonstration of training and testing samples from two subjects.

A. Best Sensor Location

Judging from the EER of the same posture and signal processing method, we discover that either the heart or the sternum is the most appropriate location to place the accelerometer for authentication. Moreover, the vertical and dorsal-ventral accelerations are more reliable than the horizontal orientation. Ranking afterwards is the left carotid, at which the vertical acceleration appears to be the most suitable biometric. Placing the sensor on the wrists gives rise to the worst authentication performance. Nevertheless, in the walking motion without robust signal processing, we notice that the vertical acceleration from the right hand wrist shows the lowest EER compared to all other accelerations. This could possibly imply that the walking pattern is recognized in the hand waving movement.

B. Best Posture

Among the four activities, standing results into the optimal posture for authentication, following by post-exercise, sitting, and walking. The lowest EER for each of these activities are 0.01%, 0.02%, 0.98%, and 4.18%, respectively. The results

TABLE II
EQUAL ERROR RATE OF THE SCG-BASED BIOMETRIC MODELS

Sensor Location & Acceleration Axis	Sit EER	Resilient Sit EER	Stand EER	Resilient Stand EER	Walk EER	Resilient Walk	Post-exercise EER	Resilient Post-exercise EER
Right Hand Vertical	0.45	0.14	0.47	0.15	0.35	0.25	0.45	0.20
Right Hand Horizontal	0.49	0.17	0.47	0.19	0.50	0.29	0.48	0.19
Right Hand Dorsal-Ventral	0.49	0.18	0.47	0.15	0.52	0.23	0.49	0.18
Left Hand Vertical	0.47	0.16	0.47	0.13	0.52	0.26	0.47	0.13
Left Hand Horizontal	0.48	0.17	0.48	0.18	0.51	0.29	0.48	0.19
Left Hand Dorsal-Ventral	0.46	0.13	0.47	0.20	0.48	0.21	0.47	0.20
Left Carotid Vertical	0.43	0.09	0.40	0.06	0.49	0.19	0.41	0.09
Left Carotid Horizontal	0.43	0.13	0.47	0.15	0.49	0.25	0.45	0.12
Left Carotid Dorsal-Ventral	0.46	0.12	0.45	0.14	0.49	0.23	0.48	0.11
Heart Vertical	0.28	0.01	0.28	0.01	0.44	0.06	0.30	<0.001
Heart Horizontal	0.37	0.05	0.35	0.003	0.45	0.13	0.37	0.02
Heart Dorsal-Ventral	0.33	0.02	0.26	<0.001	0.41	0.06	0.31	0.02
Sternum Vertical	0.27	0.01	0.28	0.003	0.45	0.06	0.31	<0.001
Sternum Horizontal	0.36	0.04	0.33	0.006	0.43	0.14	0.36	0.02
Sternum Dorsal-Ventral	0.32	0.01	0.28	0.003	0.41	0.04	0.31	0.01

could probably imply that both large and restricted motions like walking and sitting would lead to worse authentication models. On the contrary, standing normally and sitting post-exercise are relatively natural posture for the human participants. Therefore, we spot better SCG-based biometric authentication models in these two postures.

C. Efficacy of the Motion Artifact Resilient Method

Owing to the fact that SCG is susceptible to motion artifact [9], [10], we propose the motion artifact removal strategy and showcase its efficacy in Table II. For all the experiments, the robustness enhanced biometric authentication models are favored.

TABLE III
COMPARISON OF SCG EER TO STATE OF THE ART

Method	EER (%)	Posture
PCA on SCG [7]	not reported	unmentioned
Wavelet Transform SCG [8]	< 0.01	supine
Ours - vertical SCG	0.98	Sitting
Ours - dorsal-ventral SCG	0.01	Standing
Ours - sternum dorsal-ventral SCG	4.18	Walking
Ours - sternum vertical SCG	0.02	Post-exercise

D. Comparison with the State-of-the-Art Works

We compare our SCG-based biometric authentication models with other existing studies in Table III. We display the competency of the proposed models in allowing the motions generated by the human body. Although the EER is not lower than the supine SCG, we still present < 1% EER in sitting, post-exercise sitting, and standing positions. Furthermore, we demonstrate that our model is able to handle walking SCG and leverage it as a biometric.

IV. CONCLUSIONS

We demonstrate that seismocardiogram could be a promising biometric even with a person in motions. Through the exploration of tri-axial accelerations of different body parts,

we reveal that placing the accelerometer near the heart or the sternum produces robust signals for biometric authentication. Moreover, we exhibit that standing is the most appropriate posture for biometric authentication compared to sitting and walking. Based on our findings, we believe that SCG biometric is worth exploring, and we are eager to identify the characteristic points in SCG under motion that distinguish between individuals in the future.

REFERENCES

- [1] T. Ko, "Multimodal biometric identification for large user population using fingerprint, face and iris recognition," in *AIPR*. IEEE, 2005, pp. 6–pp.
- [2] Z. Zhao, Y. Zhang, Y. Deng, and X. Zhang, "Ecg authentication system design incorporating a convolutional neural network and generalized s-transformation," *Computers in biology and medicine*, vol. 102, pp. 168–179, 2018.
- [3] O. T. Inan, P.-F. Migeotte, K.-S. Park, M. Etemadi, K. Tavakolian, R. Casanella, J. Zanetti, J. Tank, I. Funtova, G. K. Prisk, *et al.*, "Ballistocardiography and seismocardiography: A review of recent advances," *JBHI*, vol. 19, no. 4, pp. 1414–1427, 2014.
- [4] P.-Y. Hsu, P.-H. Hsu, and H.-L. Liu, "Fold electrocardiogram into a fingerprint," in *IEEE CVPR Workshops*, 2020, pp. 828–829.
- [5] M. Merone, P. Soda, M. Sansone, and C. Sansone, "Ecg databases for biometric systems: A systematic review," *Expert Systems with Applications*, vol. 67, pp. 189–202, 2017.
- [6] B. Wu, G. Yang, L. Yang, and Y. Yin, "Robust ecg biometrics using two-stage model," in *2018 24th International Conference on Pattern Recognition (ICPR)*. IEEE, 2018, pp. 1062–1067.
- [7] A. A. Bui, Z. Yu, and F. M. Bui, "A biometric modality based on the seismocardiogram (scg)," in *IEMCON*. IEEE, 2015, pp. 1–7.
- [8] P.-Y. Hsu, P.-H. Hsu, and H.-L. Liu, "Exploring scg biometrics with wavelet transform," in *ICPR*. IEEE, 2021, pp. 4450–4457.
- [9] A. Taebi, B. E. Solar, A. J. Bomar, R. H. Sandler, and H. A. Mansy, "Recent advances in seismocardiography," *Vibration*, vol. 2, no. 1, pp. 64–86, 2019.
- [10] E. Chang, C.-K. Cheng, A. Gupta, P.-H. Hsu, P.-Y. Hsu, H.-L. Liu, A. Moffitt, A. Ren, I. Tsaor, and S. Wang, "Cuff-less blood pressure monitoring with a 3-axis accelerometer," in *EMBC*. IEEE, 2019, pp. 6834–6837.
- [11] K. Pandia, S. Ravindran, R. Cole, G. Kovacs, and L. Giovangrandi, "Motion artifact cancellation to obtain heart sounds from a single chest-worn accelerometer," in *ICASSP*. IEEE, 2010, pp. 590–593.
- [12] O. T. Inan, M. Etemadi, R. M. Wiard, L. Giovangrandi, and G. Kovacs, "Robust ballistocardiogram acquisition for home monitoring," *Physiological measurement*, vol. 30, no. 2, p. 169, 2009.